

N2SID: Nuclear Norm Subspace Identification [★]

Michel Verhaegen ^a Anders Hansson ^b

^a*Delft Center for Systems and Control
Delft University
Delft, The Netherlands*

^b*Division of Automatic Control
Linköping University
Linköping, Sweden*

Abstract

The identification of multivariable state space models in innovation form is solved in a subspace identification framework using convex nuclear norm optimization. The convex optimization approach allows to include constraints on the unknown matrices in the data-equation characterizing subspace identification methods, such as the lower triangular block-Toeplitz of weighting matrices constructed from the Markov parameters of the unknown observer. The classical use of instrumental variables to remove the influence of the innovation term on the data equation in subspace identification is avoided. The avoidance of the instrumental variable projection step has the potential to improve the accuracy of the estimated model predictions, especially for short data length sequences. This is illustrated using a data set from the DaSIy library. An efficient implementation in the framework of the Alternating Direction Method of Multipliers (ADMM) is presented that is used in the validation study.

Key words: Subspace system identification, Nuclear norm optimization, Rank constraint, Short data batches, Alternating Direction Method of Multipliers

1 Introduction

The generation of Subspace IDentification (SID) methods for the identification of Linear Time-Invariant (LTI) state space models as developed originally in [20, 10, 21] derive *approximate* models rather than models that are “optimal” with respect to a goodness of fit criterium defined in terms of the weighted norm of the difference between the measured output and the model predicted output. The approximation is based on linear algebra transformations and factorizations of structured Hankel matrices constructed from the input-output data that are related via the so-called *data equation* [25]. All existing SID methods aim to derive a low rank matrix from which key subspaces, hence the name subspace identification, are derived. The low rank approximation is in general done using a Singular Value Decomposition (SVD).

A number of recent developments have been made to integrate the low rank approximation step in SID with a goodness of fit into a single multi-criteria convex optimization problem. These contributions were inspired by the work in [3] to approximate a constraint on the rank of a matrix by minimizing its nuclear norm. It resulted into a number of improvements to the low rank approximation step over the classically used SVD in SID, [12, 13, 16, 5, 7, 11, 18, 19].

When considering identifying innovation state space models, a common approach is to make use of instrumental variables [7]. It is well known that the projection operation related to the use of instrumental variables may result into a degradation of the accuracy of the estimated quantities.

In this paper we present a new SID method for identifying multivariable state space models in innovation form within the framework of nuclear norm optimization. The new SID method avoids the use of instrumental variables. The method is a convex relaxation of Pareto optimization in which structural constraints are imposed on the unknowns in the data equation, such as their block-Toeplitz matrix structure. This Pareto optimization ap-

[★] Part of the research was done while the first author was a Visiting Professor at the Division of Automatic Control, Department of Electrical Engineering, Linköping University, Sweden. This work was partially supported by the European Research Council Advanced Grant Agreement No. 339681. Corresponding Author: m.verhaegen@tudelft.nl.

proach allows to make a trade-off between a Prediction Error type of optimality criteria, that is minimizing the (co-)variance of the one-step ahead prediction of a linear Kalman filter type observer, on one hand, and finding an observer of lowest complexity, i.e. of lowest model order, on the other hand. A key result is that the structural Toeplitz constraint is sufficient to find the minimal observer realization when the optimal one-step ahead prediction of the output is known. The incentive to estimate a Kalman filter type of observer also justifies the constraint to attempt to minimize the variance of the one-step ahead prediction error.

It is interesting to note that this key result stipulates precise conditions on the persistency of excitation of the input (in open-loop experiments). For many instrumental variable based SID methods it is still an open question what the persistency of excitation condition is on a generic input sequence to guarantee the algorithm to work for finite data length samples or to be consistent [9].

The convex relaxation of the new SID approach is denoted by Nuclear Norm Subspace IDentification (N2SID). Its advantages are demonstrated in a comparison study on real-life data sets in the DaSIy data base, [2]. In this comparison study N2SID demonstrated to yield models that lead to improved predictions over two existing SID methods, N4SID and the recent Nuclear Norm based SID methods presented in [11] and with the Prediction Error Method (PEM) [15]. For the sake of brevity the results about only one data set are reported. For more information on a more extensive experimental analysis leading to similar conclusions we refer to [24].

The foundations for N2SID were presented in [23]. There the resulting optimization problem was solved using a Semi-Definite Programming (SDP) solver after a reformulation of the problem into an equivalent SDP problem. In addition to this the problem formulation was approximated in order to obtain a problem of manageable size for current SDP solvers. In this paper we will instead solve the problem with the Alternating Direction Method of Multipliers (ADMM). ADMM is known to be a good choice for solving regularized nuclear norm problems as the ones we are solving in this paper, [11]. In order to get an efficient implementation we have customized the computations for obtaining the coefficient matrix of the normal equations associated with our formulation using Fast Fourier Transformation (FFT) techniques. This is the key to obtain an efficient implementation.

The paper is organized as follows. In Section 2 the identification problem for identifying a multi-variable state space model in a subspace context while taking a prediction error cost function into consideration is presented. The data equation and necessary preliminaries on the assumptions made in the analysis and description of the

subspace identification method is presented in Section 3. The multi-criteria optimization problem, the analysis of the uniqueness of solution and its convex relaxation are presented in Section 4. In Section 5 we explain how to obtain an efficient ADMM code. The results of the performances are illustrated in Section 6 in a comparison study of N2SID with two other SID methods, N4SID and the recent Nuclear Norm based SID methods presented in [11] and with PEM. Finally, we end this paper with some concluding remarks.

1.1 Notations

We introduce the Matlab-like notation that for a vector or matrix $X \in \mathbb{R}^{M \times N}$ ($\mathbb{C}^{M \times N}$) it holds that $X_{m:n,p:q}$ is the sub-matrix of X with rows m through n and columns p through q . If one of the dimensions of the matrix is n , then $1 : n$ can be abbreviated as just $:$. Moreover, with $X_{m:-1:n,p:q}$ is meant the sub-matrix of X obtained by taking rows m through n in reverse order, where m is greater than or equal to n . Similar notation may be used for the columns.

2 The Subspace Identification Problem

In system identification a challenging problem is to identify Linear Time Invariant (LTI) systems with multiple inputs and multiple outputs using short length data sequences. Taking process and measurement noise into consideration, a general state space model for LTI systems can be given in so-called innovation form, [25]:

$$\begin{cases} x(k+1) = Ax(k) + Bu(k) + Ke(k) \\ y(k) = Cx(k) + Du(k) + e(k) \end{cases} \quad (1)$$

with $x(k) \in \mathbb{R}^n, y(k) \in \mathbb{R}^p, u(k) \in \mathbb{R}^m$ and $e(k)$ a zero-mean white noise sequence. Since we are interested in short data sets no requirement on consistency is included in the following problem formulation.

Problem Formulation: Given the input-output (i/o) data batches $\{u(k), y(k)\}_{k=1}^N$, with $N > n$ and assumed to be retrieved from an identification experiment with a system belonging to the class of LTI systems as represented by (1), the problem is to determine approximate system matrices $(\hat{A}_T, \hat{B}_T, \hat{C}_T, \hat{D}, \hat{K}_T)$ that define the \hat{n} -th order observer of “low” complexity:

$$\begin{cases} \hat{x}_T(k+1) = \hat{A}_T \hat{x}_T(k) + \hat{B}_T u_v(k) + \hat{K}_T (y_v(k) - \hat{C}_T \hat{x}_T(k)) \\ \hat{y}_v(k) = \hat{C}_T \hat{x}_T(k) + \hat{D} u_v(k) \end{cases} \quad (2)$$

such that the approximated output $\hat{y}_v(k)$ is “close” to the measured output $y_v(k)$ of the validation pair

$\{u_v(k), y_v(k)\}_{k=1}^{N_v}$ as expressed by a small value of the cost function,

$$\frac{1}{N_v} \sum_{k=1}^{N_v} \|y_v(k) - \hat{y}_v(k)\|_2^2. \quad (3)$$

The quantitative notions like “low” and “close approximation” will be made more precise in the new N2SID solution toward this problem. The solution to this problem is provided under 2 Assumptions. The first is listed here, the second at the end of Section 3.

Assumption A.1. The pair (A, C) is observable and the pair $(A, \begin{bmatrix} B & K \end{bmatrix})$ is reachable.

A key starting point in the formulation of subspace methods is the relation between structured Hankel matrices constructed from the i/o data. This relationship will as defined in [25] be the data equation. It will be presented in the next section.

3 The Data Equation, its structure and Preliminaries

Let the LTI model (1) be represented in its so-called observer form:

$$\begin{cases} x(k+1) = (A - KC)x(k) + (B - KD)u(k) + Ky(k) \\ y(k) = Cx(k) + Du(k) + e(k) \end{cases} \quad (4)$$

We will denote this model compactly as:

$$\begin{cases} x(k+1) = \mathcal{A}x(k) + \mathcal{B}u(k) + Ky(k) \\ y(k) = Cx(k) + Du(k) + e(k) \end{cases} \quad (5)$$

with \mathcal{A} the observer system matrix $(A - KC)$ and \mathcal{B} equal to $(B - KD)$. Though this property will not be used in the sequel, the matrix \mathcal{A} can be assumed to be asymptotically stable.

For the construction of the data equation, we store the measured i/o data in block-Hankel matrices. For fixed N assumed to be larger than the order n of the underlying system, the definition of the number of block-rows fully defines the size of these Hankel matrices. Let this dimensioning parameter be denoted by s , then the Hankel matrix of the input is defined as:

$$U_{s,N} = \begin{bmatrix} u(1) & u(2) & \cdots & u(N-s+1) \\ u(2) & u(3) & & \vdots \\ \vdots & & \ddots & \\ u(s) & u(s+1) & \cdots & u(N) \end{bmatrix}. \quad (6)$$

The Hankel matrices from the output $y(k)$ and the innovation $e(k)$ are defined similarly and denoted by $Y_{s,N}$ and $E_{s,N}$, respectively. The relationship between these Hankel matrices, that readily follows from the linear model equations in (5), require the definition of the following *structured* matrices. First we define the extended observability matrix \mathcal{O}_s :

$$\mathcal{O}_s^T = \begin{bmatrix} C^T & \mathcal{A}^T C^T & \cdots & \mathcal{A}^{T^{s-1}} C^T \end{bmatrix}. \quad (7)$$

Second, we define a Toeplitz matrix from the quadruple of systems matrices $\{\mathcal{A}, \mathcal{B}, C, D\}$ as:

$$T_{u,s} = \begin{bmatrix} D & 0 & \cdots & 0 \\ C\mathcal{B} & D & & 0 \\ \vdots & & \ddots & \\ C\mathcal{A}^{s-2}\mathcal{B} & \cdots & D \end{bmatrix} \quad (8)$$

and in the same way we define a Toeplitz matrix $T_{y,s}$ from the quadruple $\{\mathcal{A}, K, C, 0\}$. Finally, let the state sequence be stored as:

$$X_N = \begin{bmatrix} x(1) & x(2) & \cdots & x(N-s+1) \end{bmatrix}. \quad (9)$$

Then the data equation compactly reads:

$$Y_{s,N} = \mathcal{O}_s X_N + T_{u,s} U_{s,N} + T_{y,s} Y_{s,N} + E_{s,N}. \quad (10)$$

This equation is a simple linear matrix equation that highlights the challenges in subspace identification, which is to approximate from the given Hankel matrices $Y_{s,N}$ and $U_{s,N}$ the column space of the observability matrix and/or that of the state sequence of the observer (5).

The equation is highly structured. In this paper we focus on the following key structural properties about the unknown matrices in (10):

- (1) The matrix product $\mathcal{O}_s X_N$ is *low rank* when $s > n$.
- (2) The matrices $T_{u,s}$ and $T_{y,s}$ are block-Toeplitz.
- (3) The matrix $E_{s,N}$ is block-Hankel.

The interesting observation is that these 3 structural properties can be added as constraints to the multi-criteria optimization problem considered while preserving convexity. This is demonstrated in Section 4.

The analysis in Section 4 requires the following preliminaries.

Definition 1 [25]: A signal $u(k) \in \mathbb{R}^m$ is *persistently exciting of order s* if and only if there exists an integer N such that the matrix $U_{s,N}$ has full row rank.

Lemma 2 [9]: Consider the state space model in innovation form (1) and let all stochastic signals be stationary and ergodic, let Assumption A.1 be satisfied and let the input $u(k)$ be quasi-stationary [15] and persistently exciting of order $s + n$, then:

$$\lim_{N \rightarrow \infty} \frac{1}{N} \begin{bmatrix} X_N \\ U_{s,N} \end{bmatrix} \begin{bmatrix} X_N^T & U_{s,N}^T \end{bmatrix} > 0$$

Corollary 3 Let the conditions stipulated in Lemma 2 hold, and let $u(k)$ be statistically independent from the innovation sequence $e(\ell)$ for all k, ℓ , then,

$$\lim_{N \rightarrow \infty} \frac{1}{N} \begin{bmatrix} X_N \\ U_{s,N} \\ Y_{s,N} \end{bmatrix} \begin{bmatrix} X_N^T & U_{s,N}^T & Y_{s,N}^T \end{bmatrix} > 0$$

Proof: Since $e(k)$ is white noise, it follows that $\mathbb{E}[x(k)e(\ell)^T] = 0$ (with \mathbb{E} denoting the expectation operator), for $\ell \geq k$. This in combination with the independency between $u(k)$ and $e(\ell)$, the white noise property of $e(k)$ and the ergodicity or the quasi-stationarity of the signals yields,

$$\lim_{N \rightarrow \infty} \frac{1}{N} \begin{bmatrix} X_N \\ U_{s,N} \\ E_{s,N} \end{bmatrix} \begin{bmatrix} X_N^T & U_{s,N}^T & E_{s,N}^T \end{bmatrix} > 0 \quad (11)$$

Considering model (1), let the block-Toeplitz matrices $T'_{u,s}$ and $T_{e,s}$ be defined as the Toeplitz matrix $T_{u,s}$ in (8) but from the quadruples (A, B, C, D) and (A, K, C, I) , respectively. Let $O_s^T = \begin{bmatrix} C^T & A^T C^T & \dots & A^{T^{s-1}} C^T \end{bmatrix}$. Then we can state the following alternative data equation:

$$Y_{s,N} = O_s X_N + T'_{u,s} U_{s,N} + T_{e,s} E_{s,N}$$

By this data equation, we have that,

$$\begin{bmatrix} X_N \\ U_{s,N} \\ Y_{s,N} \end{bmatrix} = \begin{bmatrix} I & 0 & 0 \\ 0 & I & 0 \\ O_s & T'_{u,s} & T_{e,s} \end{bmatrix} \begin{bmatrix} X_N \\ U_{s,N} \\ E_{s,N} \end{bmatrix}$$

The results follows from (11) and the fact that the matrix $T_{e,s}$ is square and invertible. \square

Based on this result the following assumption is stipulated.

Assumption A.2. Consider the model (5), then there exists an integer N such that the compound matrix,

$$\begin{bmatrix} X_N \\ U_{s,N} \\ Y_{s,N} \end{bmatrix}$$

has full row rank.

4 N2SID

4.1 Pareto optimal Subspace Identification

When assuming the optimal observer given, the quantity $\hat{y}(k)$ is the minimum variance prediction of the output and equal to $y(k) - e(k)$. Let the Hankel matrix $\hat{Y}_{s,N}$ be defined from this sequence $\hat{y}(k)$ as we defined $Y_{s,N}$ from $y(k)$. Then the data equation (10) can be reformulated into:

$$\hat{Y}_{s,N} = \mathcal{O}_s X_N + T_{u,s} U_{s,N} + T_{y,s} Y_{s,N}. \quad (12)$$

Let $\mathcal{T}_{p,m}$ denote the class of lower triangular block-Toeplitz matrices with block entries $p \times m$ matrices and let \mathcal{H}_p denote the class of block-Hankel matrices with block entries of p column vectors. Then the three key structural properties listed in Section 3 are taken into account in an optimization problem seeking a trade-off between the following cost functions,

$$\begin{aligned} & \text{rank}(\Gamma_{s,N} - \Theta_u U_{s,N} - \Theta_y Y_{s,N}) \\ & \text{and } \text{Tr } \mathbb{E}[(y(k) - \gamma(k))(y(k) - \gamma(k))^T] \end{aligned} \quad (13)$$

Here \mathbb{E} denotes the expectation operator. The matrix $\Gamma_{s,N} \in \mathcal{H}_p$ is the (block-) Hankel matrix approximating the Hankel matrix $\hat{Y}_{s,N}$ and constructed from the approximation of the one-step ahead prediction of the output denoted by $\gamma(k)$ in the same way $\hat{Y}_{s,N}$ was constructed from $\hat{y}(k)$. Further, we have the following constraints on the matrices $\Theta_u \in \mathcal{T}_{p,m}$ and $\Theta_y \in \mathcal{T}_{p,p}$.

An optimal trade-off between the above two cost functions is called a Pareto optimal solution. Moreover, the Pareto optimization problem is not tractable. For that purpose we will develop in the next subsection a *convex relaxation* of the cost functions. This will make it possible to obtain all Pareto optimal solutions using scalarization.

Before stating this convex relaxation an analysis is made on the additional structure that can be imposed on the block-Toeplitz matrices Θ_u and Θ_y and/or under what conditions their block-Toeplitz structure is sufficient to find a unique solution.

4.2 Additional structure in the block-Toeplitz matrices $T_{u,s}$ and $T_{y,s}$

In this section we analyse the additional structure present in the block-Toeplitz matrices $T_{u,s}$ and $T_{y,s}$ as well as the conditions under which the block-Toeplitz structure is sufficient to find the system matrices $(\mathcal{A}_T, \mathcal{B}_T, \mathcal{C}_T, D, K_T)$. These conditions, not including the additional structural constraint highlighted in Lemma 4, is summarized in Theorem 1 of this paper.

Lemma 4 *Let $s > n$, then we can partition the block-Toeplitz matrices $T_{u,s}$ and $T_{y,s}$, defined in the data equation (10) as,*

$$T_{u,s} = \left[\begin{array}{c|c} T_{u,n} & 0 \\ \hline H_{u,s-n} & T_{u,s-n} \end{array} \right] \quad (14)$$

and likewise for the matrix $T_{y,s}$. Here the matrices $H_{u,s-n}$ and $H_{y,s-n}$ can be decomposed as,

$$\left[\begin{array}{c|c} H_{u,s-n} & H_{y,s-n} \end{array} \right] = \left[\begin{array}{c} \mathcal{C} \\ \mathcal{C}\mathcal{A} \\ \vdots \\ \mathcal{C}\mathcal{A}^{s-n-1} \end{array} \right] \left[\begin{array}{cc} \mathcal{A}^{n-1}\mathcal{B} & \dots & \mathcal{B} \\ \mathcal{A}^{n-1}\mathcal{K} & \dots & \mathcal{K} \end{array} \right] \quad (15)$$

Proof: Follows by construction. \square

Remark 5 *Lemma 4 can be used to impose an additional constraint on the block-Toeplitz matrices Θ_u and Θ_y . If we partition these block-Toeplitz matrices conformal their counterparts $T_{u,s}$ and $T_{y,s}$ as highlighted in Lemma 4, as follows,*

$$\Theta_{u,s} = \left[\begin{array}{c|c} \Theta_{u,n} & 0 \\ \hline H_{u,s-n}^\Theta & \Theta_{u,s-n} \end{array} \right]$$

(likewise for $\Theta_{y,s}$), then for the case $s \geq 2n$ we can impose the following additional constraint,

$$\text{rank} \left(\left[\begin{array}{cc} H_{u,s-n}^\Theta & H_{y,s-n}^\Theta \end{array} \right] \right) = n$$

The additional constraint highlighted in Remark 5 can be reformulated, as done e.g. in [18, 19], as a rank minimization constraint, that can be relaxed to a convex constraint using the nuclear norm. However we seek to avoid imposing this additional constraint in order to minimize the number of regularization parameters. The basis hereof is provided in the next Theorem.

Theorem 1 *Consider the observer in (1) with $x(k) \in \mathbb{R}^n$ and consider the rank optimization problem in Eq.*

(13) *only with $\Gamma_{s,N}$ fixed to $\hat{Y}_{s,N}$, let $s > n$ and let Assumptions A.1 and A.2 be satisfied, Then,*

$$\min_{\Theta_u \in \mathcal{T}_{p,m}, \Theta_y \in \mathcal{T}_{p,p}} \text{rank} \left(\hat{Y}_{s,N} - \Theta_u U_{s,N} - \Theta_y Y_{s,N} \right) = n$$

Further the arguments optimizing the above optimization problem, denoted as $\hat{\Theta}_u, \hat{\Theta}_y$ are unique and equal to,

$$\hat{\Theta}_u = T_{u,s} \quad \hat{\Theta}_y = T_{y,s}$$

with $T_{u,s}, T_{y,s}$ the true underlying block-Toeplitz matrices in the data equation(10).

Proof: Let $\delta_u \in \mathcal{T}_{p,m}, \delta_y \in \mathcal{T}_{p,p}$, then,

$$\begin{aligned} \hat{Y}_{s,N} - \Theta_u U_{s,N} - \Theta_y Y_{s,N} &= \hat{Y}_{s,N} - (T_{u,s} + \delta_u)U_{s,N} - \\ &\quad (T_{y,s} + \delta_y)Y_{s,N} \\ &= \mathcal{O}_s X_N - \delta_u U_{s,N} - \delta_y Y_{s,N} \end{aligned}$$

Therefore,

$$\begin{aligned} \text{rank} \left(\hat{Y}_{s,N} - \Theta_u U_{s,N} - \Theta_y Y_{s,N} \right) &= \\ \text{rank} \left(\mathcal{O}_s X_N - \delta_u U_{s,N} - \delta_y Y_{s,N} \right) \end{aligned}$$

Application of Sylvester's inequality [25] and under Assumption A.2, we further have,

$$\text{rank} \left(\hat{Y}_{s,N} - \Theta_u U_{s,N} - \Theta_y Y_{s,N} \right) = \text{rank} \left(\left[\begin{array}{cc} \mathcal{O}_s & \delta_u & \delta_y \end{array} \right] \right) \quad (16)$$

First notice that under Assumption A.1 the rank of this matrix is n for $\delta_u = 0$ and $\delta_y = 0$. Since the $\text{rank} \left(\left[\begin{array}{cc} \mathcal{O}_s & \delta_u & \delta_y \end{array} \right] \right) \geq \text{rank} \left(\mathcal{O}_s \right)$ for all δ_u, δ_y , we have that n is the minimal value of the rank in (16).

It will now be shown that this minimal value of the rank, can only be reached for both δ_u and δ_y equal to zero.

For that purpose, let $t = \{t_i \in \mathbb{R}^{p \times (m+p)}\}_{i=1}^s$ be a sequence of arbitrary matrices that define the lower triangular block-Toeplitz matrix $\Delta^s(t)$ as:

$$\Delta^s(t) = \left[\begin{array}{cccc} t_1 & 0 & \dots & 0 \\ & t_2 & & \vdots \\ & & \ddots & \vdots \\ & & & t_s \end{array} \right] \in \mathbb{R}^{sp \times s(m+p)}$$

The columns of the compound matrix $\left[\begin{array}{cc} \delta_u & \delta_y \end{array} \right]$ in (16) can always be permuted into a matrix of the form $\Delta^s(t)$

and since column permutations do not change the rank of a matrix we have that,

$$\text{rank}\left(\begin{bmatrix} \mathcal{O}_s & \delta_u & \delta_y \end{bmatrix}\right) = \text{rank}\left(\begin{bmatrix} \mathcal{O}_s & \Delta^s(t) \end{bmatrix}\right)$$

Now we show that the following condition

$$\text{rank}\left(\begin{bmatrix} \mathcal{O}_s & \Delta^s(t) \end{bmatrix}\right) = n$$

implies that $\Delta^s(t)$ has to be zero. In order for the above rank constraint to hold we need $\Delta^s(t)$ to be of the following form:

$$\begin{bmatrix} t_1 & 0 & \cdots & 0 & 0 \\ t_2 & t_1 & & 0 & 0 \\ \vdots & & \ddots & & \\ t_s & t_{s-1} & \cdots & t_2 & t_1 \end{bmatrix} = \mathcal{O}_s \begin{bmatrix} q_1 & q_2 & \cdots & q_{s-1} & q_s \end{bmatrix} \quad (17)$$

The fact that $s > n$, we have that $\text{rank}(\mathcal{O}_{s-1}) = n$ and therefore we can deduce from the first $p(s-1)$ rows of the last $p+m$ columns in the expression (17) that,

$$q_s = 0 \Rightarrow t_1 = 0$$

Using this result, and the Toeplitz structure of $\Delta^s(t)$, we can in the same way conclude from the first $p(s-1)$ rows and from the columns $(s-2)(m+p)+1$ to $(s-1)(m+p)$ in (17) that,

$$q_{s-1} = 0 \Rightarrow t_2 = 0 \quad \text{etc.}$$

Hence there cannot be a $\Delta^s(t)$ with the given Toeplitz structure that is different from zero such that $\text{rank}\left(\begin{bmatrix} \mathcal{O}_s & \Delta^s(t) \end{bmatrix}\right) = n$. Hence the minimal value of the rank of the matrix $\begin{bmatrix} \mathcal{O}_s & \delta_u & \delta_y \end{bmatrix}$ in (16) w.r.t. δ_u, δ_y yields zero value of both. This concludes the proof. \square

4.3 A convex relaxation

A convex relaxation of the NP hard problem formulation in (13) will now be developed. The original problem is reformulated in two ways. First, the rank operator is substituted by the nuclear norm. The nuclear norm of a matrix X denoted by $\|X\|_*$ is defined as the sum of the singular values of the matrix X . It is also known as the trace norm, the Ky Fan norm or the Schatten norm, [14]. This is known to be a good approximation of the rank operator when it is to be minimized, [4, 3]. Second, the minimum variance criterium is substituted by the following sample average $\frac{1}{N} \sum_{k=1}^N \|y(k) - \gamma(k)\|_2^2$.

By introducing a scalarization parameter $\lambda \in [0, \infty)$, which can be interpreted as a regularization parameter,

all Pareto optimal solutions of the convex reformulation of the N2SID problem can be obtained by solving:

$$\min_{\Gamma_{s,N} \in \mathcal{H}_p, \Theta_{u,s} \in \mathcal{T}_{p,m}, \Theta_{y,s} \in \mathcal{T}_{p,p}} \|\Gamma_{s,N} - \Theta_{u,s}U_{s,N} - \Theta_{y,s}Y_{s,N}\|_* + \frac{\lambda}{N} \sum_{k=1}^N \|y(k) - \gamma(k)\|_2^2 \quad (18)$$

for all values of $\lambda \in [0, \infty)$.

Remark 4 *The method can be extended to other related identification problems. For example one way to consider the identification problem of an innovation model with absence of a measurable input, is to consider the following convex relaxed problem formulation:*

$$\min_{\Gamma_{s,N} \in \mathcal{H}_p, \Theta_{y,s} \in \mathcal{T}_{p,p}} \|\Gamma_{s,N} - \Theta_{y,s}Y_{s,N}\|_* + \frac{\lambda}{N} \sum_{k=1}^N \|y(k) - \gamma(k)\|_2^2. \quad (19)$$

It is well-known that the problem (18) can be recast as a Semi-Definite Programming (SDP) problem, [4, 3], and hence it can be solved in polynomial time with standard SDP solvers. The reformulation, however, introduces additional matrix variables of dimension $N \times N$, unless the problem is not further approximated using randomization techniques as in [23]. In section 5 we will present an alternative exact method using ADMM inspired by its successful application in [11].

4.4 Calculation of the system matrices

The convex-optimization problem (18) yields the estimates of the quantities $\Gamma_{s,N}$, $\Theta_{u,s}$ and $\Theta_{y,s}$. Since the outcome depends on the regularization parameter λ , let us denote these estimates as $\hat{\Gamma}_{s,N}(\lambda)$, $\hat{\Theta}_{u,s}(\lambda)$ and $\hat{\Theta}_{y,s}(\lambda)$ respectively. The determination of the system matrices starts with an SVD of the “low rank” approximated matrix as follows:

$$\hat{\Gamma}_{s,N}(\lambda) - \hat{\Theta}_{u,s}(\lambda)U_{s,N} - \hat{\Theta}_{y,s}(\lambda)Y_{s,N} = \begin{bmatrix} U_{\hat{n}}(\lambda) & | & \star \end{bmatrix} \begin{bmatrix} \Sigma_{\hat{n}}(\lambda) & | & 0 \\ 0 & | & \star \end{bmatrix} \begin{bmatrix} V_{\hat{n}}^T(\lambda) \\ \star \end{bmatrix} \quad (20)$$

where \hat{n} is an integer denoting the \hat{n} largest singular values and the notation \star denotes a compatible matrix not of interest here. The selection of \hat{n} is outlined in the algorithmic description given next.

The algorithm requires in addition to the input-output data sequences the user to specify the parameter s to fix the number of block rows in the block-Hankel matrices $U_{s,N}$ and $Y_{s,N}$ and an interval for the parameter λ denoted by $\Lambda = [\lambda_{\min}, \lambda_{\max}]$. As for the implementation described in [11], which we will refer to as **WNNopt**, the identification data set could be partitioned in two parts. The first part is referred to as the **ide-1** part of

the identification data set and the remaining part of the identification data set is referred to as the **ide-2** part. This splitting of the data set was recommended in [11] to avoid overfitting. In the *N2SID* algorithm three variants can be substituted in the algorithmic block 'compute $\mathcal{M}_j(\lambda)$ ' for $j = 1, 2, 3$. This algorithmic block performs the actual calculation of the one-step ahead predictor and the three variants are summarized after the description of the core part of *N2SID*.

N2SID algorithm:

Grid the interval $\Lambda = [\lambda_{\min}, \lambda_{\max}]$ in N different points, e.g. using the Matlab

notation $\Lambda = \text{logspace}(\log(\lambda_{\min}), \log(\lambda_{\max}), L)$

for $i=1:L$,

Solve (18) for $\lambda = \Lambda(i)$ and data set ide-1.

Compute the SVD as in (20) for $\lambda = \Lambda(i)$.

Select Select the model order \hat{n} from the singular values in (20). This can be done manually by the user or automatically. Such automatic selection can be done as in the *N4SID* implementation in [15] as highlighted in [11]: order the singular values in (20) in descending order, then select that index of the singular value that in logarithm is closest to the logarithmic mean of the maximum and minimum singular values in (20).

Compute system matrices $\{\hat{\mathcal{A}}_T, \hat{\mathcal{B}}_T, \hat{\mathcal{C}}_T, \hat{\mathcal{D}}, \hat{K}_T\}$ according to the procedure 'Compute $\mathcal{M}_j(\lambda)$ ' for $j = 1, 2, 3$ and $\lambda = \Lambda(i)$.

Using the estimated system matrices $\{\hat{\mathcal{A}}_T, \hat{\mathcal{B}}_T, \hat{\mathcal{C}}_T, \hat{\mathcal{D}}\}$, and the validation data in ide-2, compute the simulated output $\hat{y}(k, \lambda)$ as,

$$\begin{aligned}\hat{x}_T(k+1) &= \hat{\mathcal{A}}_T \hat{x}_T(k) + \hat{\mathcal{B}}_T u(k) \\ \hat{y}(k, \lambda) &= \hat{\mathcal{C}}_T \hat{x}_T(k) + \hat{\mathcal{D}} u(k)\end{aligned}\quad (21)$$

and evaluate the cost function,

$$J(\lambda) = \sum_{i=1}^N \|y(k) - \hat{y}(k, \lambda)\|_2^2$$

end

Select $\mathcal{M}_j(\lambda_{\text{opt}})$ with λ_{opt} given as:

$$\lambda_{\text{opt}} = \min_{\lambda \in \Lambda} J(\lambda)$$

The subsequent three ways to compute the model are summarized as:

Compute $\mathcal{M}_1(\lambda)$:

STEP 1: From the SVD in (20), and the selected model order \hat{n} , the pair $\hat{\mathcal{A}}_T, \hat{\mathcal{C}}_T$ is derived from the matrix

$U_{\hat{n}}$ as done in classical SID methods by considering $U_{\hat{n}}$ to be an approximation of the extended observability matrix \mathcal{O}_s , see e.g. [25].

STEP 2: With $U_{\hat{n}}$ and the estimated matrix $T_{y,s}^e$ we exploit that the latter matrix approximates the block-Toeplitz matrix $T_{y,s}$ to estimate the observer gain \hat{K}_T via the solution of a standard linear least squares problem. This is seen as follows. Let us assume the block Toeplitz matrix $T_{y,s}$ be given and denoted explicitly as,

$$T_{y,s} = \begin{bmatrix} 0 & 0 & \cdots & 0 & 0 \\ CK & 0 & & 0 & 0 \\ CAK & CK & & 0 & 0 \\ \vdots & & & \ddots & \\ CA^{s-2}K & \cdots & CK & 0 \end{bmatrix}$$

If we know the matrix \mathcal{O}_s , we can write the following set of equations,

$$\mathcal{O}_s(1 : (s-1)p, :)K = T_{y,s}(p+1 : ps, 1 : p)$$

Let us now denote the first $(s-1)p$ rows of the matrix $U_{\hat{n}}(\lambda_i)$ by $\hat{\mathcal{O}}_{s-1,T}$ and let us denote the submatrix of the matrix $\hat{\Theta}_{y,s}(\lambda_i)$ from rows $p+1$ to row ps and from column 1 to p by $\hat{T}_{y,s}(p+1 : ps, 1 : p)$, then we can estimate K_T from:

$$\min_{K_T} \|\hat{\mathcal{O}}_{s-1,T} K_T - \hat{T}_{y,s}(p+1 : ps, 1 : p)\|^2 \quad (22)$$

This estimate of the observer gain is used to estimate the system matrix A_T as:

$$\hat{A}_T = \hat{\mathcal{A}}_T + \hat{K}_T \hat{\mathcal{C}}_T \quad (23)$$

STEP 3: Let the approximation of the observer be denoted as:

$$\begin{aligned}\hat{x}_T(k+1) &= \hat{\mathcal{A}}_T \hat{x}_T(k) + \hat{\mathcal{B}}_T u(k) + \hat{K}_T y(k) \\ \hat{y}(k) &= \hat{\mathcal{C}}_T \hat{x}_T(k) + \hat{\mathcal{D}} u(k)\end{aligned}\quad (24)$$

Then the estimation of the pair $\hat{\mathcal{B}}_T, \hat{\mathcal{D}}$ and the initial conditions of the above observer can again be done via a linear least squares problem as outlined in [25] by minimizing the RMS value of the prediction error $y(k) - \hat{y}(k)$ determined from the identification data in **ide-1**. The estimated input matrix \hat{B}_T is then determined as:

$$\hat{B}_T = \hat{\mathcal{B}}_T + \hat{K}_T \mathcal{D} \quad (25)$$

Compute $\mathcal{M}_2(\lambda)$:

STEP 1: as in *Compute* $\mathcal{M}_1(\lambda)$.

STEP 2: Derive an estimate of the state sequence of the observer (24) from the SVD (20), where for the

sake of compactness again the system symbol $\hat{x}_T(k)$ will be used,

$$\begin{bmatrix} \hat{x}_T(1) & \hat{x}_T(2) & \cdots & \hat{x}_T(N-s+1) \end{bmatrix} \approx V_{\hat{n}}^T(\lambda)$$

Using the singular values this approximation could also be scaled as $\sqrt{\Sigma_{\hat{n}}(\lambda)}V_{\hat{n}}^T(\lambda)$.

STEP 3: Knowledge of the estimated state sequence of the observer (24) turns the estimation of the system matrices $\hat{A}_T, \hat{B}_T, \hat{C}_T, \hat{D}, \hat{K}_T$ and the observer initial conditions into linear least squares problem. The estimated pair (\hat{A}_T, \hat{B}_T) can be computed from this quintuple as outlined in (23) and (25), respectively.

Compute $\mathcal{M}_3(\lambda)$:

STEP 1 and 2: as in *Compute $\mathcal{M}_1(\lambda)$* .

STEP 3: With $U_{\hat{n}}$ and the estimated Markov parameters in $T_{u,s}^e$ we could similarly to estimating the Kalman gain, also estimate the pair \hat{B}_T, \hat{D} via a linear least squares problem. The matrix \hat{B}_T can be estimated from \hat{B}_T as outlined in (25),

In the experiments reported in Section 6 use will be made of N2SID Algorithm with the model computation block *Compute $\mathcal{M}_1(\lambda)$* . It turned out that the N2SID algorithm is much less sensitive to overparametrization compared as compared to WNNopt. For that reason we will use the whole identification data set in all steps of the N2SID algorithm for the experiments reported in Section 6, i.e. **ide-1** and **ide-2** are identical and equal to the identification data set.

5 ADMM

The problem we like to solve is exactly of the form in (20) in [11], i.e.

$$\min_x \|\mathcal{A}(x) + A_0\|_* + \frac{1}{2}(x - a)^T H(x - a) \quad (26)$$

for some linear operator $\mathcal{A}(x)$ and some positive semidefinite matrix H . In the above mentioned reference the linear operator is a Hankel matrix operator, and this structure is used to tailor the ADMM code to run efficiently. Essentially the key is to be able to compute the coefficient matrix related to the normal equations of the linear operator in an efficient way using FFT. This matrix M is defined via

$$\mathcal{A}_{\text{adj}}(\mathcal{A}(x)) = Mx, \forall x$$

where $\mathcal{A}_{\text{adj}}(\cdot)$ is the adjoint operator of $\mathcal{A}(\cdot)$. Similar techniques have been used for Toeplitz operators in [17], and are closely related to techniques for exploiting Toeplitz structure in linear systems of equations, [6].

For our problem the linear operator consists of a sum of Hankel and Toeplitz operators, and we will show how FFT techniques can be used also for this operator. For more details on the ADMM algorithm see the appendix.

5.1 Circulant, Toeplitz and Hankel Matrices

We define the circulant matrix operator $\mathcal{C}^n : \mathbb{R}^n \rightarrow \mathbb{R}^{n \times n}$ of a vector $x \in \mathbb{R}^n$ via

$$\mathcal{C}^n(x) = \begin{bmatrix} x_1 & x_n & \cdots & x_3 & x_2 \\ x_2 & x_1 & x_n & & \\ \vdots & x_2 & x_1 & \ddots & \vdots \\ x_{n-1} & & \ddots & \ddots & x_n \\ x_n & x_{n-1} & \cdots & x_2 & x_1 \end{bmatrix}. \quad (27)$$

We also define the Hankel matrix operator $\mathcal{H}^{(m,n)} : \mathbb{R}^{m+n-1} \rightarrow \mathbb{R}^{m \times n}$ of a vector $x \in \mathbb{R}^{m+n-1}$ via

$$\mathcal{H}^{(m,n)}(x) = \begin{bmatrix} x_1 & x_2 & \cdots & x_n \\ x_2 & \ddots & & \vdots \\ \vdots & & & \vdots \\ x_m & \cdots & \cdots & x_{m+n-1} \end{bmatrix}. \quad (28)$$

For a vector $x \in \mathbb{R}^{m+n-1}$ it holds that $\mathcal{H}^{(m,n)}(x) = \mathcal{C}_{n:n+m-1,n:-1:1}^{m+n-1}(x)$, i.e. the Hankel operator is the lower left corner of the circulant operator where the columns are taken in reverse order. We also define the Toeplitz operator $\mathcal{T}^n : \mathbb{R}^{2n-1} \rightarrow \mathbb{R}^{n \times n}$ of a vector $x \in \mathbb{R}^{2n-1}$ via

$$\mathcal{T}^n(x) = \begin{bmatrix} x_n & x_{n-1} & \cdots & x_1 \\ x_{n+1} & \ddots & & \vdots \\ \vdots & & \ddots & \vdots \\ x_{2n-1} & \cdots & \cdots & x_n \end{bmatrix}. \quad (29)$$

We realize that $\mathcal{T}^n(x) = \mathcal{H}_{:,n:-1:1}^{(n,n)}(x)$, i.e. a Toeplitz operator can be obtained from a square Hankel operator by taking the columns in reverse order. We are finally interested in upper triangular Toeplitz operators with and without zeros on the diagonal, and we remark that these are easily obtained from the normal Toeplitz operator by replacing x with $\begin{bmatrix} x^T & 0 \end{bmatrix}^T$, which will be upper triangular with a non-zero diagonal if $x \in \mathbb{R}^n$ and with a zero diagonal if $x \in \mathbb{R}^{n-1}$.

5.2 The Fourier Transform and Hankel Matrices

It is well-known, [6], that if we let $\mathcal{F}^n \in \mathbb{C}^{n \times n}$ be the discrete Fourier transform matrix of dimension n , then

the circulant matrix can be expressed as

$$\mathcal{C}^n(x) = \frac{1}{n}(\mathcal{F}^n)^H \text{diag}(\mathcal{F}^n x) \mathcal{F}^n. \quad (30)$$

From this we immediately obtain that the Hankel matrix can be expressed as

$$\mathcal{H}^{(m,n)}(x) = \frac{1}{N} H^H \text{diag}(\mathcal{F}^N x) G \quad (31)$$

where $N = n + m - 1$, $F = \mathcal{F}^N$, $G = F_{:,n:-1:1}$ and $H = F_{:,n:n+m-1}$. This expression will make it easy for us to represent the adjoint of the Hankel operator. It is straight forward to verify that the adjoint $\mathcal{H}_{\text{adj}}^{(m,n)}(Z) : \mathbb{R}^{m \times n} \rightarrow \mathbb{R}^{n+m-1}$ is given by

$$\mathcal{H}_{\text{adj}}^{(m,n)}(Z) = \frac{1}{N} F^H \text{diag}(H Z G^H).$$

Notice that we are abusing the operator $\text{diag}(\cdot)$. In case the argument is a vector the operator produces a diagonal matrix with the vector on the diagonal, and in case the argument is a square matrix, the operator produces a vector with the components equal to the diagonal of the matrix.

5.3 The Linear Operator \mathcal{A}

We will now present the linear operator that we are interested in for the SISO case: $\mathcal{A} : \mathbb{R}^N \times \mathbb{R}^s \times \mathbb{R}^{s-1} \rightarrow \mathbb{R}^{s \times n}$, where

$$\mathcal{A}(x) = \mathcal{H}^{(s,n)}(\hat{y}) + \mathcal{T}^s \left(\begin{bmatrix} v_{s:-1:1} \\ 0 \end{bmatrix} \right)^T V + \mathcal{T}^s \left(\begin{bmatrix} w_{s-1:-1:1} \\ 0 \end{bmatrix} \right)^T W$$

where $n = N - s + 1$, $x = (\hat{y}, v, w)$ with $\hat{y} \in \mathbb{R}^N$, $v \in \mathbb{R}^s$, $w \in \mathbb{R}^{s-1}$, $V \in \mathbb{R}^{s \times N}$, and $W \in \mathbb{R}^{s \times N}$. By taking $V = -U_{s,N}$ and $W = -Y_{s,N}$ we obtain the linear operator for N2SID. Then, v and w are the first columns of the Toeplitz matrices $T_{u,s}$ and $T_{y,s}$, respectively. We can express $\mathcal{A}(x)$ in terms of Hankel operators as:

$$\mathcal{A}(x) = \mathcal{H}^{(s,n)}(\hat{y}) + \mathcal{H}_{:,s:-1:1}^{(s,s)} \left(\begin{bmatrix} v_{s:-1:1} \\ 0 \end{bmatrix} \right)^T V + \mathcal{H}_{:,s-1:-1:1}^{(s,s)} \left(\begin{bmatrix} w_{s-1:-1:1} \\ 0 \end{bmatrix} \right)^T W.$$

The adjoint of this operator can be expressed in terms of the adjoint of the Hankel operator as

$$\mathcal{A}_{\text{adj}}(Z) = \begin{bmatrix} \mathcal{H}_{\text{adj}}^{(s,n)}(Z) \\ \mathcal{H}_{\text{adj},s:-1:1}^{(s,s)}(V Z_{s:-1:1,:}^T) \\ \mathcal{H}_{\text{adj},s-1:-1:1}^{(s,s)}(W Z_{s-1:-1:1,:}^T) \end{bmatrix}$$

5.4 Forming the Coefficient Matrix

A key matrix in the ADDM algorithm is the matrix M defined via

$$\mathcal{A}_{\text{adj}}(\mathcal{A}(x)) = Mx, \quad \forall x.$$

We will now show how this matrix can be formed efficiently using the Fast Fourier Transform (FFT). We partition the matrix as

$$M = \begin{bmatrix} M_{11} & M_{12} & M_{13} \\ M_{12}^T & M_{22} & M_{23} \\ M_{13}^T & M_{23}^T & M_{33} \end{bmatrix}$$

where the partition is done to conform with the partition $x = (y, v, w)$. It is then clear that M_{11} is defined via

$$\mathcal{H}_{\text{adj}}^{(s,n)}(\mathcal{H}^{(s,n)}(y)) = M_{11}y, \quad \forall y$$

The left hand side can be expressed as

$$\frac{1}{N^2} F^H \text{diag}(H H^H \text{diag}(F y) G G^H).$$

From the identity

$$\text{diag}(A \text{diag}(x) B) = (A \odot B^T)x$$

where \odot denotes the Hadamard product of matrices, it follows that

$$M_{11} = \frac{1}{N^2} F^H \left((H H^H) \odot (\overline{G G^H}) \right) F$$

The efficient way to form M_{11} is to first compute F, G and H using an FFT algorithm, and then to form the matrix

$$X = (H H^H) \odot (\overline{G G^H}).$$

After this one should apply the inverse FFT algorithm to X^T , and then to the transpose of the resulting matrix once more the inverse FFT algorithm.

The expressions for the other blocks of the matrix M can be derived in a similar way, and they are given by:

$$\begin{aligned} M_{12} &= \frac{1}{N^2} F^H \left((H_{:,s:-1:1} H^H) \odot (\overline{G V^T G_{:,1:s}^H}) \right) F_{:,s:-1:1} \\ M_{13} &= \frac{1}{N^2} F^H \left((H_{:,s:-1:1} H^H) \odot (\overline{G W^T G_{:,1:s}^H}) \right) F_{:,s-1:-1:1} \\ M_{22} &= \frac{1}{\kappa^2} F_{:,s:-1:1}^H \left((H V V^H H^H) \odot (\overline{G G^H}) \right) F_{:,s:-1:1} \\ M_{23} &= \frac{1}{\kappa^2} F_{:,s:-1:1}^H \left((H V W^H H^H) \odot (\overline{G G^H}) \right) F_{:,s-1:-1:1} \\ M_{33} &= \frac{1}{\kappa^2} F_{:,s-1:-1:1}^H \left((H W W^H H^H) \odot (\overline{G G^H}) \right) F_{:,s-1:-1:1}. \end{aligned}$$

Notice that for the last three blocks the matrices F , G , and H are defined via a discrete Fourier transform matrix of order $\kappa = 2s - 1$.

5.5 MIMO Systems

So far we have only discussed SISO systems. For a general $p \times m$ system we may write the linear operator $\mathcal{A} : \mathbb{R}^{pN} \times \mathbb{R}^{pms} \times \mathbb{R}^{pp(s-1)} \rightarrow \mathbb{R}^{ps \times n}$ as:

$$\mathcal{A}(x) = \sum_{i=1}^p \mathcal{A}_i(x_i) \otimes e_i$$

where

$$\begin{aligned} \mathcal{A}_i(x_i) = & \mathcal{H}^{(s,n)}(\hat{y}_i) + \sum_{j=1}^m \mathcal{H}_{:,s:-1:1}^{(s,s)} \left(\begin{bmatrix} v_{s:-1:1}^{i,j} \\ 0 \end{bmatrix} \right)^T V_j \\ & + \sum_{j=1}^p \mathcal{H}_{:,s-1:-1:1}^{(s,s)} \left(\begin{bmatrix} w_{s-1:-1:1}^{i,j} \\ 0 \end{bmatrix} \right)^T W_j \end{aligned}$$

where $V_j = -U_{s,N}^j$ and $W_j = -Y_{s,N}^j$ are Hankel matrices defined from u_j and y_j , i.e. from the j th inputs and outputs, respectively, and where e_i is the i th basis vector. Hence we may interpret each term $\mathcal{A}_i(x_i)$ as defining a MISO system in the sense that each predicted output can be written as a linear combination of all the inputs and outputs. If we write the adjoint variable Z in a similar way as $Z = \sum_{i=1}^p Z_i \otimes e_i$, it follows that the adjoint operator is given by $\mathcal{A}_{\text{adj}}(Z) = (\mathcal{A}_{\text{adj},1}(Z_1), \dots, \mathcal{A}_{\text{adj},p}(Z_p))$. Hence the matrix M will now be blockdiagonal with blocks defined from the identity

$$\mathcal{A}_{\text{adj},i}(\mathcal{A}_i(x_i)) = M_i x_i, \quad \forall x_i, i = 1, \dots, p.$$

It is not difficult to realize that the operators $\mathcal{A}_{\text{adj},i}(Z_i)$ will be given by

$$\mathcal{A}_{\text{adj},i}(Z_i) = \begin{bmatrix} \mathcal{H}_{\text{adj}}^{(s,n)}(Z_i) \\ \mathcal{H}_{\text{adj},s:-1:1}^{(s,s)}(V_1 Z_{i;s:-1:1,:}^T) \\ \vdots \\ \mathcal{H}_{\text{adj},s:-1:1}^{(s,s)}(V_m Z_{i;s:-1:1,:}^T) \\ \mathcal{H}_{\text{adj},s-1:-1:1}^{(s,s)}(W_1 Z_{i;s:-1:1,:}^T) \\ \vdots \\ \mathcal{H}_{\text{adj},s-1:-1:1}^{(s,s)}(W_p Z_{i;s:-1:1,:}^T) \end{bmatrix}.$$

Hence each of the blocks M_i will have a similar structure as the M matrix for the SISO system. However, the sub-blocks M_{12} , M_{13} , M_{22} , M_{23} and M_{33} will have sub-blocks themselves reflecting that fact that there are several inputs and outputs. M_{11} will be the same as M_1

for the SISO case for all i . Below are formulas given for sub-blocks of each of the other matrices

$$\begin{aligned} M_{12j} &= \frac{1}{N^2} F^H \left((H_{:,s:-1:1} H^H) \odot (\overline{GV_j^T G_{:,1:s}^H}) \right) F_{:,s:-1:1} \\ M_{13j} &= \frac{1}{N^2} F^H \left((H_{:,s:-1:1} H^H) \odot (\overline{GW_j^T G_{:,1:s}^H}) \right) F_{:,s-1:-1:1} \\ M_{22jk} &= \frac{1}{\kappa^2} F_{:,s:-1:1}^H \left((HV_j V_k^H H^H) \odot (\overline{GG^H}) \right) F_{:,s:-1:1} \\ M_{23jk} &= \frac{1}{\kappa^2} F_{:,s:-1:1}^H \left((HV_j W_k^H H^H) \odot (\overline{GG^H}) \right) F_{:,s-1:-1:1} \\ M_{33jk} &= \frac{1}{\kappa^2} F_{:,s-1:-1:1}^H \left((HW_j W_k^H H^H) \odot (\overline{GG^H}) \right) F_{:,s-1:-1:1}. \end{aligned}$$

It is interesting to notice that these formulas do not depend on index i . This means that all M_i are the same.

6 Validation Study

In this section we report results on numerical experiments using real-life data sets. We will make use of some representative data sets from the DaISy collection, [2]. For preliminary test with the new N2SID method based on academic examples, we refer to [23].

The numerical results reported in Subsection 6.3 were performed with Matlab. The implementations have been carried out in MATLAB R2013b running on an Intel Core i7 CPU M 250 2 GHz with 8 GB of RAM.

6.1 Data selection and pre-processing

From the DaISy collection, [2], five representative data sets were selected. These sets contain SISO, SIMO, MISO and MIMO systems. Information about the selected data sets is provided in Table 1. In order to evaluate the performances for small length data sets, data sets of increasing length are considered. The data length is indicated by N_{ide} in Table 2 for each data set of Table 1. To test the sensitivity of the identification methods with respect to the length of the identification data set, N_{ide} is increased from a small number, as compared to the total number of samples available, in a way as indicated in Table 2. From each identification and validation data set the offset is removed. Data set 2 from the continuous stirred tank reactor is scaled in such a way that both outputs have about the same numerical range. This is achieved by scaling the detrended versions of these outputs such that the maximum value of each output equals 1.

Since many of the data sets contain poorly excited data at their beginning, the first del samples are discarded from each data set. The actual value of del for each data set is listed in Table 2. Finally each identified model is validated for each test case on the same validation data set. These validation data sets contain the N_{val} samples

Table 1

Five benchmark problems from the DaISy collection, [2]; N_{tot} is the total number of data samples available

Nr	Data set	Description	Inputs	Outputs	N_{tot}
1	96-007	CD player arm	2	2	2048
2	98-002	Continuous stirring tank reactor	1	2	7500
3	96-006	Hair dryer	1	1	1000
4	97-002	Steam heat exchanger	1	1	4000
5	96-011	Heat flow density	2	1	1680

Table 2

The increasing length N_{ide} of the data sets used for system identification starting with the sample index del ; N_{val} indicates the length of the validation data set starting with the sample index $\max(N_{\text{ide}}) + 1$.

Nr	N_{ide}										del	N_{val}
1	80	120	150	175	200	300	400	500	600		120	500
2	100	150	200	300	400	500	600	700	800		200	1500
3	80	100	120	140	160	180	200	250	300	400	120	600
4	150	200	300	500	750	1000	1250	1500	1750		200	1500
5	175	200	250	300	350	400	450	500	550	600	200	1000

following the sample with index $\max(N_{\text{ide}}) + 1$. The value of N_{val} is listed in Table 2.

6.2 Compared Identification methods

Three SID methods are compared in the tests. Their key user selection parameters are listed in Table 3. One of the key user selection parameters of the SID methods is the number of block rows s of the Hankel data matrices. In methods like N4SID or WNNopt of Table 3 a distinction could be made in the number of block rows of so-called future and past Hankel matrices. Such differentiation is not necessary for the N2SID algorithm. Since such differentiation is still an open research problem we opted in this simulation study to take the number of block rows of the future and past Hankel matrices in N4SID or WNNopt equal to the number of block rows in the N2SID algorithm. Table 3 also lists the interval of the regularization parameter λ to be specified for the Nuclear Norm based methods.

For N4SID we further used the default settings except that the Kalman filter gain is not estimated, a guaranteed stable simulation model is identified, no input delays are estimated and these are fixed to zero, and finally no covariance estimates are determined. The order selection is done with N4SID using the option 'best', [15]. This results in a similar automatic choice as we have implemented for N2SID.

For WNNopt in [11] the weighting according to the CVA method is used. Also here no Kalman gain is estimated and the input delay is set to zero. As indicated in [11] an 'identification' and a 'validation' data set is needed to perform the selection of the regularization parameter λ

in order to avoid overfitting. In this paper both data sets are retrieved from the identification data set of length N_{ide} by splitting it into two almost equal parts differing in length by at most one sample.

For N2SID we used the ADMM algorithm presented in [11], where we have provided our own routines for computing M as explained in section 5. As explained in [11] we also make use of simultaneous diagonalization of M and the positive semidefinite matrix H in (26) in order not to have to make different factorizations for each value of the regularization parameter λ . The maximum number of iterations in the ADMM algorithm have been set to 200, the absolute and relative solution accuracy tolerances have been set to 10^{-6} , and 10^{-3} , respectively. The parameters used to update the penalty parameter have been set to $\tau = 2$ and $\mu = 10$. We label our N2SID Algorithm with N2SID). Also we do not split the data for N2SID. We have also carried out experiments when we did split the data. This resulted in most cases in comparable results and in some cases even better results.

The SID methods are compared with the prediction error method PEM of the matlab System Identification toolbox [15]. Here the involvement of the user in specifying the model structure is avoided by initializing PEM with the model determined by N4SID. Therefore, the model order of PEM is the same as that determined by the N4SID method. In this way no user selection parameters are needed to be specified for PEM. This is in agreement with the recommendation given on the PEM help page <http://nf.nci.org.au/facilities/software/Matlab/toolbox/ident/pem.html> when identifying black-box state space models.

Table 3

Three SID methods and their user selection parameters $\frac{\lambda}{N_{\text{ide}}}$ and the number of block-rows in the data Hankel matrices s .

Method	$\frac{\lambda}{N_{\text{ide}}}$	s	Weighting
N4SID [[15]]	/	15	automatic
WNNopt, [[11]]	$[10^{-3}, 10^3]$	15	CVA
N2SID Algorithm	$[10^{-1.5}, 10^3]$	15	/

6.3 Results and Discussion

The three SID methods in Table 3 and the PEM method will be compared for the data sets in Table 1. The results of this comparison are for each data set summarized in two graphs in the same figure. The left graph of the figure displays the goodness of fit criterium VAF. This is defined using the identified quadruple of system matrices $[\hat{A}_T, \hat{B}_T, \hat{C}_T, \hat{D}]$ obtained with each method to predict the output using the validation data set. Let the predicted output be denoted by $\hat{y}_v(k)$ for each method, and let the output measurement in the validation data set be denoted by $y_v(k)$. Then VAF is defined as:

$$\text{VAF} = \left(1 - \frac{\frac{1}{N_{\text{val}}} \sum_{k=1}^{N_{\text{val}}} \|y_v(k) - \hat{y}_v(k)\|_2^2}{\frac{1}{N_{\text{val}}} \|y_v(k)\|_2^2}\right) 100\% \quad (32)$$

The right graph of the figure displays the model complexity as defined by the model order of the state space model. Both the goodness of fit and estimated model order are graphed versus the length of the identification data batch as indicated by the symbol N_{ide} in Table 2.

All these results are obtained in a similar “automized manner” for fair comparison as outlined in section 6.2. In order to evaluate the results additional information is retrieved from the singular values as computed by the SID methods WNNopt and N2SID. This is done in order to see possible improvements in the low rank detection by the new SID method N2SID over WNNopt. For an illustration of the potential improvement of the latter over N4SID we refer to [11].

6.3.1 The CD player arm data set (# 1 in Table 1)

The results are summarized in Figure 1. The goodness of fit is given on the left side of this figure and the detected order \hat{n} on the right side. For $N_{\text{ide}} \leq 400$, N2SID outperforms all other methods and it was always better than N4SID. PEM is able to improve the results of N4SID in most cases. Its results remain however inferior to N2SID. In general N2SID detects a larger model order. For the shortest data lengths $N_{\text{ide}} = 80$ and 120, WNNopt was not able to produce results since for that case the ADMM implementation broke down. The reason being that the Schur form was no longer computable as it contained NaN numbers. For that reason both the VAF and the order were put to zero. The WNNopt determined for $150 \leq N_{\text{ide}} \leq 300$ a lower model order \hat{n} compared to

N2SID, but this at the cost of a lower VAF. For $N_{\text{ide}} = 150$ and 175, the same order as for N4SID was detected, however with worse VAF as compared to both N4SID and PEM. For $N_{\text{ide}} \geq 400$ the limit set on the model order, which was 10 in all experiments, was selected by WNNopt, sometimes but not always yielding a better VAF.

The effect of the use of instrumental variables and the splitting of the identification data set to avoid overfitting on the order selection is clear from the singular values of N2SID and WNNopt given in Figure 2 for $N_{\text{ide}} = 600$. This plot visually supports the selection of a 7-th order model by N2SID and it also explains why WNNopt selects a larger model order. One possible explanation is that the instrumental variables and projections have “projected away” crucial information in the data.

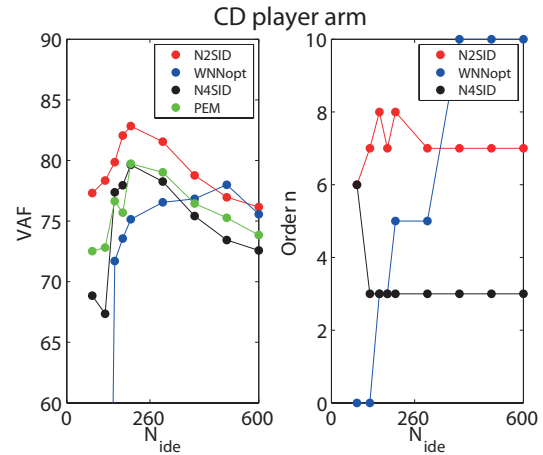


Fig. 1. VAF Daisy # 1 - CD player arm.

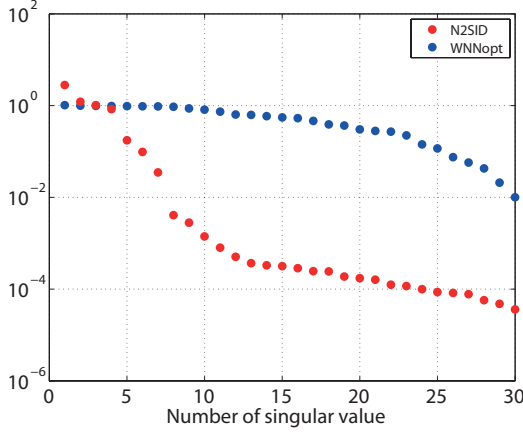


Fig. 2. Singular values Daisy # 1 - CD player arm.

6.3.2 The Continuous stirred Tank Reactor data set (# 2 in Table 1)

The goodness of fit parameter VAF and the estimated model order \hat{n} are plotted in Figure 3 in the left and right graphs, respectively. For $N_{ide} = 100$ and 150 WNNopt was not able to provide numerical results. For that reason the corresponding VAF values are again fixed to zero. PEM resulted in bad VAF results for $N_{ide} = 100$, probably as a consequence of bad initialization from N4SID. However, also for $N_{ide} = 800$ PEM had severely degraded results despite the fact that N4SID provided a model of comparable quality with the other SID methods.

The singular values in Figure 4 indicate that for $N_{ide} = 800$ both N2SID and WNNopt have the same order estimate \hat{n} . There is a clear gap in the singular values for WNNopt. The difference in detected order despite similar VAF indicates that order detection is not so critical for this example.

6.3.3 The Hair dryer data set (# 3 in Table 1)

The goodness of fit parameter VAF and the estimated model order \hat{n} are plotted in Figure 5 in the left and right graphs, respectively. Here it is again clear that N2SID outperforms all other SID methods and provides more stable behavior when increasing N_{ide} compared to the

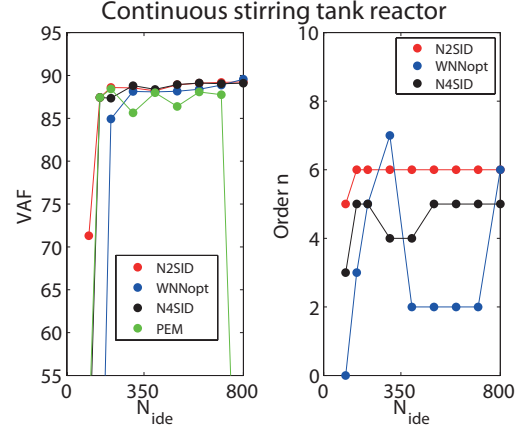


Fig. 3. VAF Daisy # 2 - Continuous Stirred Tank Reactor.

fluctuating behavior of the other methods, both with respect to VAF and estimated model order. WNNopt fails to address the case of very small data length sets, i.e. when $N_{ide} = 80$ and 100. The combination of N4SID and PEM enables in a number of cases to provide models with a similar VAF compared to N2SID and in a small number of cases to slightly improve the results over N2SID. However, this is not consistent, since for $N_{ide} = 400$ the VAF is worsened compared to the initialization with N4SID.

Figure 6 displays the singular values for the last data set where $N_{ide} = 400$ in Figure 6. It confirms the improved potential in low rank approximation by N2SID over WNNopt. The latter method diminishes the gap, leading in general to a larger model order estimation. This larger model order does however for this example not lead to a better output prediction.

6.3.4 The Steam Heat Exchanger data set (# 4 in Table 1)

The goodness of fit parameter VAF and the estimated model order \hat{n} are plotted in Figure 7.

N2SID again for small data sets with N_{ide} ranging between 150 and 750 yields the best output predictions of all methods. Comparing the VAF value in Figure 7 with those for the previous Daisy data sets reveals that the

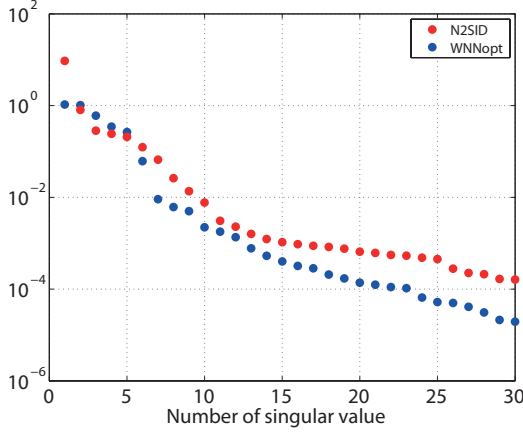


Fig. 4. Singular values Daisy # 2 - Continuous Stirred Tank Reactor.

values are smaller. This reflects problems with the data set due to lower signal to noise ratio, system nonlinearity, etc. Because of this we started the analysis with the smallest value of N_{ide} equal to 150, since for smaller values poor results were obtained for all methods.

The other methods show a similar behavior as for the previously analysed data sets: in most cases but not all PEM improves over N4SID, WNNopt displays inferior behavior for $N_{ide} \leq 1250$, and both N2SID and N4SID (PEM) determine a smaller order than WNNopt.

Finally, the plot of the singular values for the last data set in Figure 8 displays a similar behavior. Both singular value plots clearly support the automatic order selection made. However N2SID has a better trade-off between model complexity and model accuracy as expressed by the VAF.

6.3.5 Heat flow density data set (# 5 in Table 1)

The goodness of fit parameter VAF and the estimated model order \hat{n} are plotted in Figure 9.

For this data set WNNopt provides for $200 \leq N_{ide} \leq 450$ the best results but in general detects a larger model order. For the smallest length data set WNNopt produced

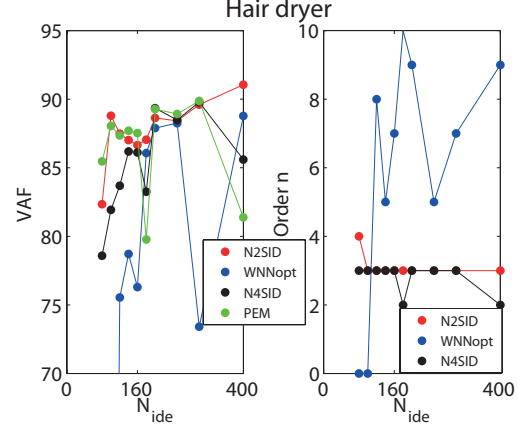


Fig. 5. VAF Daisy # 3 - Hair dryer.

inferior VAF. N2SID provides a better VAF prediction compared to N4SID and PEM and this for a smaller model order \hat{n} as compared to WNNopt.

From the singular values in Figure 10 for $N_{ide} = 600$ an order selection of 1 up to 4 is clearly justified by N2SID. The order selection made by WNNopt is much less clear.

6.3.6 General Observation from the analysed Daisy data sets.

The automatized analysis of the 5 Daisy data sets clearly demonstrates the merit of the new SID method N2SID over the other representative identification methods considered. Especially when considering data sets of *small length* it is able to make a good and sometimes excellent trade-off between model complexity and model accuracy as expressed by the goodness of fit. The improvement over the other analysed nuclear norm subspace identification method WNNopt in order detection both in revealing a clear gap as well as in detecting models of low complexity is evident.

7 Concluding Remarks

Subspace identification of multivariable state space innovation models is revisited in this paper in the scope

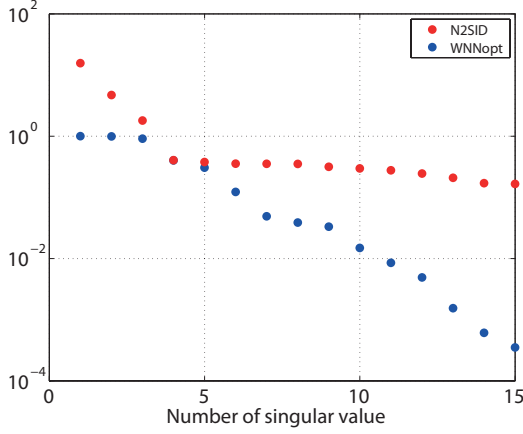


Fig. 6. Singular values Daisy # 3 - Hair dryer.

of nuclear norm optimization methods and using the observer form. A new subspace identification method is presented, referred to as N2SID. N2SID is the first subspace identification method that addresses the identification of innovation state space models *without* the use of instrumental variables (IVs). The avoidance of using IVs leads to a number of improvements. First as shown in the experimental study in [24], it leads to improved results in identifying innovation models when compared to existing SID methods, like N4SID and the recent Nuclear Norm based SID methods presented in [11] and with the Prediction Error Method (PEM) [15]. This improvement especially holds for small length data batches, i.e. when the number of samples is only a small multiple of the order of the underlying system. Second, as illustrated by Theorem 1, the methodology presented enables to provide insight on the necessary conditions of persistency of excitation of the input on the existence of a unique solution. Finally, the new N2SID methodology will enable to address other interesting identification problems in a subspace identification framework, such as the identification of distributed systems as shown in [26, 27, 22].

Acknowledgement: The authors kindly acknowledge Mr. Baptiste Sinquin from Ecole Centrale Lyon for his help in a preliminary matlab comparison study with N2SID during his internship at the Delft Center for Systems and Control under the supervision of Prof. M. Verhaegen. Also the discussions

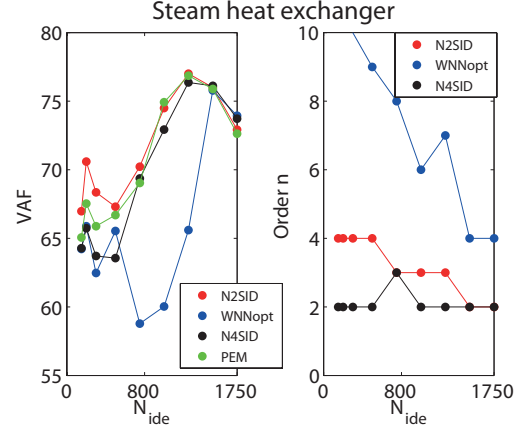


Fig. 7. VAF Daisy # 4 - Steam Heat Exchanger.

with Dr. Chengpu Yu of the Delft Center for Systems and Control on the topic of Theorem 1 are very much appreciated.

The authors express their full appreciation for the constructive comments raised by the anonymous reviewers.

References

- [1] S. Boyd, N. Parikh, E. Chu, B. Peleato, and J. Eckstein. Distributed optimization and statistical learning via the alternating direction method of multipliers. *Foundations and Trends in Machine Learning*, 3(1):1–122, 2011. Michael Jordan, Editor in Chief.
- [2] B. De Moor, P. De Gersem, B. De Schutter, and W. Favoreel. DAISY: A database for the identification of systems. *Journal A: Special Issue on CACSD (Computer Aided COntrol System Design)*, 38(3):4–5, Sep. 1997.
- [3] M. Fazel. *Matrix Rank Minimization with Applications*. PhD thesis, Stanford University, 2002.
- [4] M. Fazel, H. Hindi, and S. Boyd. A rank minimization heuristic with application to minimum order system approximation. In *Proceedings of the American Control Conference*, pages 4734–4739, 2001.
- [5] M. Fazel, T. K. Pong, D. Sun, and P. Tseng. Hankel matrix rank minimization with applications to

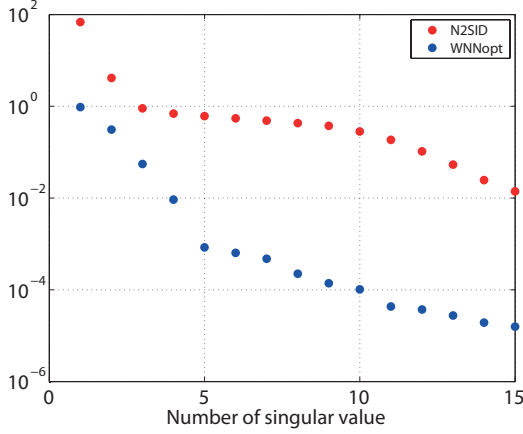


Fig. 8. Singular values Daisy # 4 - Steam Heat Exchanger.

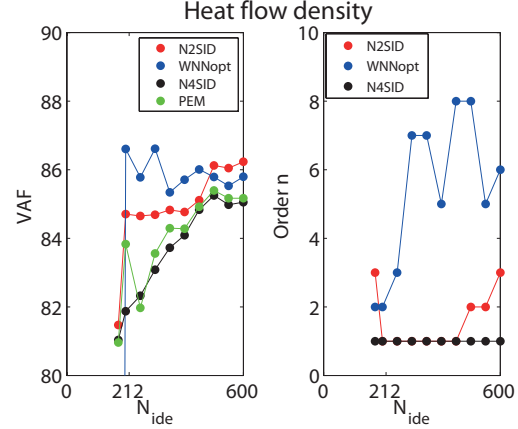


Fig. 9. VAF Daisy # 5 -Heat flow density.

system identification and realization. *SIAM Journal on Matrix Analysis and Applications*, 34(3):946–977, 2013.

- [6] G. H. Golub and Ch. F. van Loan. *Matrix Computations*. The Johns Hopkins University Press, Baltimore, Maryland, 1996. Third Edition.
- [7] A. Hansson, Z. Liu, and L. Vandenberghe. Subspace system identification via weighted nuclear norm optimization. In *Proceedings of the 51st IEEE Conference on Decision and Control*, pages 3439–3444, 2012.
- [8] B. S. He, H. Yang, and S. L. Wang. Alternating direction method with self adaptive penalty parameters for monotone variational inequalities. *Journal of Optimization Theory and Applications*, 106(2):337–356, 2000.
- [9] M. Jansson and B. Wahlberg. On consistency of subspace methods for system identification. *Automatica*, 34(12):1507–1519, 1998.
- [10] W.E. Larimore. Canonical variate analysis in identification, filtering, and adaptive control. In *Proceedings of the 29th IEEE Conference on Decision and Control, 1990.*, pages 596–604 vol.2, 1990.
- [11] Z. Liu, A. Hansson, and L. Vandenberghe. Nuclear norm system identification with missing inputs and outputs. *Systems & Control Letters*, 62:605–612, 2013.
- [12] Z. Liu and L. Vandenberghe. Interior-point method

for nuclear norm approximation with application to system identification. *SIAM Journal on Matrix Analysis and Applications*, 31(3):1235–1256, 2009.

- [13] Z. Liu and L. Vandenberghe. Semidefinite programming methods for system realization and identification. In *Proceedings of the Joint 48th IEEE Conference on Decision and Control and 28th Chinese Control Conference*, pages 4676–4681, 2009.
- [14] Z. Liu and L. Vandenberghe. Interior-point method for nuclear norm approximation with application to system identification. *SIAM Journal on Matrix Analysis and Applications*, 31(3):1235–1256, 2010.
- [15] L. Ljung. *System Identification Toolbox for use with MATLAB. Version 7*. The MathWorks, Inc, Natick, MA, 7th edition, 2007.
- [16] K. Mohan and M. Fazel. Reweighted nuclear norm minimization with application to system identification. In *Proceedings of American Control Conference*, pages 2953–2959, 2010.
- [17] T. Roh and L. Vandenberghe. Discrete transforms, semi-definite programming, sum-of-squares representations of nonnegative polynomials. *SIAM Journal on Optimization*, 16(4):939–964, 2006.
- [18] R.S. Smith. Frequency domain subspace identification using nuclear norm minimization and hankel matrix realizations. *IEEE-TAC*, 59(11):2886 – 2896, 2012.
- [19] R.S. Smith. Nuclear norm minimization methods

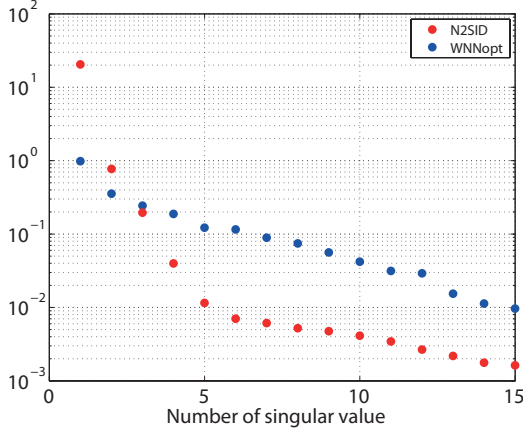


Fig. 10. Singular values Daisy # 5 - Heat flow density.

for frequency domain subspace identification. In *Proceedings of the American Control Conference*, pages 2689 – 2694, 2012.

- [20] P. Van Overschee and B. De Moor. N4sid: Subspace algorithms for the identification of combined deterministic-stochastic systems. *Automatica*, 30(1):75 – 93, 1994.
- [21] M. Verhaegen. Identification of the deterministic part of mimo state space models given in innovations form from input-output data. *Automatica*, 30(1):61 – 74, 1994.
- [22] M. Verhaegen. System identification for high resolution optical imaging, 2015. Plenary talk at IFAC Symposium SYSID. Beijing.
- [23] M. Verhaegen and A. Hansson. Nuclear norm subspace identification (n2sid) for short data batches. In *Proceedings of the 19th World Congress IFAC*, pages 9528–9533, Cape Town, South Africa, 2014.
- [24] M. Verhaegen and A. Hansson. N2sid: Nuclear norm subspace identification. *CoRR*, abs/1401.4273, 2015.
- [25] M. Verhaegen and V. Verdult. *Filtering and Identification: A Least Squares Approach*. Cambridge University Press, 2007.
- [26] C. Yu and M. Verhaegen. Local subspace identification of distributed homogeneous systems with general interconnection patterns. In *IFAC Symposium SYSID. Beijing*, pages 585–589, 2015.

Table 4
ADMM algorithm

1. Initialize x, X, Z, ρ . For example, set $x = 0, X = A_0, Z = 0, \rho = 1$.
2. Update $x := \operatorname{argmin}_{\hat{x}} L_\rho(\hat{x}, X, Z)$. See (37).
3. Update $X := \operatorname{argmin}_{\hat{X}} L_\rho(x, \hat{X}, Z)$. See (39).
4. Update $Z := Z + \rho(\mathcal{A}(x) + A_0 - X)$.
5. Terminate if $\|r_p\|_F \leq \epsilon_p$ and $\|r_d\|_2 \leq \epsilon_d$ (see (40)–(43)). Otherwise, go to step 2.

- [27] C. Yu, M. Verhaegen, and A. Hansson. Subspace identification of local 1d homogeneous systems. In *IFAC Symposium SYSID. Beijing*, pages 886–890, 2015.

Appendix: ADMM Algorithm

We here state the ADMM algorithm for a generic nuclear norm optimization problem with a quadratic regularization term:

$$\text{minimize } \|\mathcal{A}(x) + A_0\|_* + \frac{1}{2}(x - a)^T H(x - a). \quad (33)$$

The presentation is an allmost exact citation from [11]. The variable is a vector $x \in \mathbb{R}^n$. The first term in the objective is the nuclear norm of a $p \times q$ matrix $\mathcal{A}(x) + A_0$ where $\mathcal{A} : \mathbb{R}^n \rightarrow \mathbb{R}^{p \times q}$ is a linear mapping. The parameters in the second, quadratic, term in the objective of (33) are a vector $a \in \mathbb{R}^n$ and a positive semidefinite matrix $H \in \mathbb{S}^n$.

To derive the ADMM iteration we first write (33) as

$$\begin{aligned} &\text{minimize } \|X\|_* + (1/2)(x - a)^T H(x - a) \\ &\text{subject to } \mathcal{A}(x) + A_0 = X \end{aligned}$$

with two variables $x \in \mathbb{R}^n$ and $X \in \mathbb{R}^{p \times q}$. The *augmented Lagrangian* for this problem is

$$L_\rho(x, X, Z) = \|X\|_* + \frac{1}{2}(x - a)^T H(x - a) \quad (34)$$

$$+ \operatorname{Tr}(Z^T(\mathcal{A}(x) + A_0 - X)) \quad (35)$$

$$+ \frac{\rho}{2}\|\mathcal{A}(x) + A_0 - X\|_F^2, \quad (36)$$

where ρ is a positive penalty parameter. Each iteration of the ADMM consists of a minimization of L_ρ over x , a minimization of L_ρ over X , and a simple update of the dual variable Z . This is summarized in Table 4.

The update in step 2 requires the solution of a linear equation, since $L_\rho(\hat{x}, X, Z)$ is quadratic in \hat{x} . Setting the gradient of $L_\rho(\hat{x}, X, Z)$ with respect to \hat{x} equal to zero

gives the equation

$$(M + \rho H)\hat{x} = \mathcal{A}_{\text{adj}}(\rho X + \rho A_0 - Z) + Ha \quad (37)$$

where \mathcal{A}_{adj} is the adjoint of the mapping \mathcal{A} and M is the positive semidefinite matrix defined by the identity

$$Mz = \mathcal{A}_{\text{adj}}(\mathcal{A}(z)) \quad \forall z. \quad (38)$$

The minimizer X in step 4 is obtained by soft-thresholding the singular values of the matrix $\mathcal{A}(x) + A_0 + Z/\rho$:

$$\underset{\hat{X}}{\operatorname{argmin}} L_\rho(\hat{X}, x, Z) = \sum_{i=1}^{\min\{p,q\}} \max\{0, \sigma_i - \frac{1}{\rho}\} u_i v_i^T \quad (39)$$

where u_i, v_i, σ_i are given by a singular value decomposition

$$\mathcal{A}(x) + A_0 + \frac{1}{\rho}Z = \sum_{i=1}^{\min\{p,q\}} \sigma_i u_i v_i^T.$$

The residuals and tolerances in the stopping criterion in step 5 are defined as follows [1]:

$$r_p = \mathcal{A}(\mathbf{x}) + A_0 - X \quad (40)$$

$$r_d = \rho \mathcal{A}_{\text{adj}}(X_{\text{prev}} - X) \quad (41)$$

$$\epsilon_p = \sqrt{pq} \epsilon_{\text{abs}} + \epsilon_{\text{rel}} \max\{\|\mathcal{A}(x)\|_F, \|X\|_F, \|\mathcal{A}_0\|_F\} \quad (42)$$

$$\epsilon_d = \sqrt{n} \epsilon_{\text{abs}} + \epsilon_{\text{rel}} \|\mathcal{A}_{\text{adj}}(Z)\|_2, \quad (43)$$

Typical values for the relative and absolute tolerances are $\epsilon_{\text{rel}} = 10^{-3}$ and $\epsilon_{\text{abs}} = 10^{-6}$. The matrix X_{prev} in (41) is the value of X in the previous iteration.

Instead of using a fixed penalty parameter ρ , one can vary ρ to improve the speed of convergence. An example of such a scheme is to adapt ρ at the end of each ADMM iteration as follows [8]

$$\rho := \begin{cases} \tau \rho & \|r_p\|_F > \mu \|r_d\|_2 \\ \rho / \tau & \|r_d\|_2 > \mu \|r_p\|_F \\ \rho & \text{otherwise.} \end{cases}$$

This scheme depends on parameters $\mu > 1, \tau > 1$ (for example, $\mu = 10$ and $\tau = 2$). Note that varying ρ has an important consequence on the algorithm in Table 4. If ρ is fixed, the coefficient matrix $H + \rho M$ in the equation (37) that is solved in step 2 of each iteration is constant throughout the algorithm. Therefore only one costly factorization of $H + \rho M$ is required. If we change ρ after step 6, a new factorization of $H + \rho M$ is needed before returning to step 3. I explain in [11] how the extra cost of repeated factorizations can be avoided.